Electrolyte effects on bilayer tubule formation by a diacetylenic phospholipid

J. S. Chappell and P. Yager
Molecular Bioengineering Program, Center for Bioengineering, FL-20, University of Washington, Seattle, Washington 98195 USA

ABSTRACT A general effect by dissolved electrolytes to destabilize the curvature of bilayer tubules prepared from the diacetylenic phospholipid, 1,2-*bis*(10,12-tricosadiynoyl)-*sn*-gylycero-3-phosphocholine is not found. This observation discounts the role of an electrostatic interaction between polarization charges on the edges of a ferroelectric bilayer as a means by which the cylindrical curvature may be stabilized in these structures (de Gennes, P. G. 1987. *C. R. Acad. Sci. Paris.* 304:259–263). The solution-mediated ionic interactions of electrolytes with this phospholipid appear not to influence significantly the relative stability of the crystalline state of the tubule, but at high levels of a few salts, may affect the nucleation and growth of the crystalline bilayer. Curvature of the bilayer in these tubular structures apparently derives from an interaction that is not very sensitive to the presence of electrolytes. Cylindrical curvature may alternatively arise from a bending force within the bilayer that is intrinsic to the anisotropic packing of the lipid molecules (Helfrich, W., and J. Prost. 1988. *Phys. Rev.* A38:3065–3068; Chappell, J. S., and P. Yager. 1991. *Chem. Phys. Lipids.* In press), and may therefore be largely determined by the packing interactions within the hydrophobic region of the tubular bilayer.

INTRODUCTION

The formation of tubular microstructures by chiral lipid bilayers has been observed in recent years for a small group of chemically dissimilar amphiphilic molecules. Bilayer tubules were first observed upon gradually cooling liposomes produced from the diacetylenic phospholipid 1,2-*bis*(10,12-tricosadiynoyl)-*sn*-gylycero-3-phosphocholine ($DC_{8,9}PC$) below the chain melting transition of the bilayer (Yager and Schoen, 1984). The liposomes converted into hollow tubules of ~ 1 μm diam, and were composed of several concentric bilayers with evidence of long-range order or crystallinity to the molecular packing (Yager et al., 1985; Rhodes et al., 1988). Shortly thereafter, some glutamate-based amphiphiles were found to produce single bilayers in the form of helically wound ribbons of generally smaller diameter (0.01–1 μm) (Nakashima et al., 1984, 1985; Yamada et al., 1984), which eventually developed into seamless tubules from an apparent growth in the ribbon width (Nakashima et al., 1985). Subsequently, helical as well as tubular bilayer structures of $DC_{8,9}PC$ have been precipitated from ethanolic solutions of the lipid upon the addition of water (Georger et al., 1987). Similar forms of larger diameter (>10 μm) have also been prepared by the incubation and possible degradation of 1,2-dimyristoyl-*sn*-glycero-3-phosphocholine (Servuss, 1988), and most recently, helical and tubular microstructures with narrow diameters (~ 0.1 μm) have been produced from a galactocerebroside (Archibald, 1990).

A common observation among these lipid bilayer systems is the appearance of helically wound ribbons of bilayer that expose a considerable amount of bilayer edge to the surrounding aqueous medium. The detailed structure or molecular packing at the edge of these structures is unknown, but presumably the edge is exposed at the expense of some free energy. The helical structure may then be a metastable precursor to the tubular form because a tubule presents much less exposed edge and therefore is likely more stable than a helically wound ribbon of bilayer. Some observations indicate that the conversion to a tubule may occur via growth in the ribbon width to a point that the open gaps in the helical structure close (Nakashima et al., 1985), removing much of the exposed edge of the bilayer. The mechanisms by which the bilayer ribbon initially forms and grows are then important aspects to the formation of these structures (Yager et al., 1988). However, fundamental to the phenomenon remains the stabilization of the cylindrical curvature of the bilayer in these helical and tubular forms.

The anisotropic packing within the bilayer may play a key role in stabilizing the cylindrical curvature of these microstructures (de Gennes, 1987; Helfrich and Prost, 1988; Chappell and Yager, 1991*b*). Some packing states of a chiral lipid bilayer may undergo a spontaneous curvature due to intermolecular packing interactions that produce an intrinsic bending or torsional force within the bilayer or at an exposed edge (Helfrich, 1986; Helfrich and Prost, 1988). These theories prove difficult to verify conclusively, although their predictions concerning the helical parameters are generally consistent with

0006-3495/91/10/952/14 $2.00

the physical characteristics of the microstructures (Helfrich, 1986; Servuss, 1988). Alternatively, the crystalline packing of a chiral lipid bilayer may result in a ferroelectric state, from which polarization charges can develop at the edges of the bilayer (de Gennes, 1987). The electrostatic attraction of the charges on opposing edges of the bilayer may then induce the bilayer to buckle, and can thereby stabilize a cylindrical curvature. This effect is not very compatible with the proposition of a metastable helical precursor, however, because a helically wound ribbon with opposite charge on opposing edges is generally unstable toward spontaneously curling into a tubule with a much smaller radius (Chappell and Yager, 1991*a*). In addition, an electrostatic interaction is vulnerable to screening from dissolved electrolytes, where only dilute levels of an electrolyte are predicted to greatly attenuate an electrostatic interaction and thereby suppress bilayer curvature (de Gennes, 1987; Chappell and Yager, 1991*a*). This paper considers theoretically the precise effect of dissolved electrolytes on lipid tubule formation if bilayer curvature is stabilized by an electrostatic interaction. These predictions are then compared with experimental observations on the formation of $DC_{8,9}PC$ tubules in the presence of electrolytes to clarify the role that solution-mediated ionic interactions may actually play in lipid tubule formation.

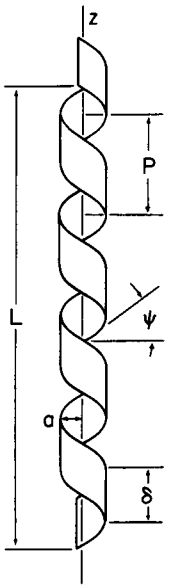

FIGURE 1 A helically wound ribbon as characterized by its radius of curvature (a), its pitch (P), and gradient angle (ψ). The dimensions of the ribbon are described by length (L) and width (δ) parameters as measured along the axis of curvature (z).

THEORY

Model

The electrostatic interactions of charges on the edges of a helically wound bilayer ribbon has been examined previously (Chappell and Yager, 1991*a*), but is briefly reviewed here for clarity. The helical conformation of the ribbon is characterized by a radius of curvature a and a gradient angle ψ, as illustrated in Fig. 1. The dimensions of the ribbon are defined by the parameters L and δ, which measure the length and width of the ribbon as projected onto the axis of curvature z. The length of one complete turn in the helix, or pitch P, is simply related to the radius and gradient angle by the expression:

$$P = 2\pi a \tan \psi. \quad (1)$$

Thus, the radius r at which a helically wound ribbon assumes a tubular form occurs at a pitch equivalent to the width parameter ($\delta = 2\pi r \tan \psi$). The gradient angle of helical bilayer structures prepared to date is generally observed to be near 45° (Nakashima et al., 1985; Servuss, 1988), and in this model, must be determined by the anisotropic properties that arise from the crystalline packing within the bilayer. This crystalline state is assumed to constrain the bilayer to curl around a single axis of curvature due to prohibitive strain for any other bending conformations of the bilayer. The anisotropic growth of the bilayer into a ribbon must then develop in the orientation that places the long dimension of the ribbon at 45° to the axis of curvature. This description appears necessary if electrostatic forces are to account for a bilayer conformed as a helically wound ribbon.

The curvature of the bilayer ribbon in this model is described by two opposing forces: an electrostatic attraction of the edge charges that induces the ribbon to curl, and an elastic strain that resists any bending of the bilayer. The electrostatic interaction arises from a ferroelectric state of the bilayer (de Gennes, 1987), whereby an electric dipole moment develops in the plane of the bilayer as a consequence of the crystalline packing, such as that found within a smectic C^* structure (de Gennes, 1974). The electric dipole effectively establishes a linear density of charge along the edges of the bilayer, which is dependent on the orientation of the dipole relative to the edge. This spatial distribution of charge is then given by the equation for a helix,

$$(x, y, z) = (a \cos t, a \sin t, at \tan \psi), \quad (2)$$

where in this parametric representation t becomes a single spatial variable along the axis of curvature.

The energy attributed to the electrostatic interactions among the edge charges is derived from Coulomb's law, where the potential energy associated with placing two

charges at a given distance of separation is,

$$E_{q,q'} = \frac{qq'}{4\pi\epsilon}\frac{1}{|\mathbf{r} - \mathbf{r}'|} \tag{3}$$

in which q and q' are the charges, $\mathbf{r}$ and $\mathbf{r}'$ are their respective position vectors, and ϵ is the dielectric constant of the surrounding medium. This energy of interaction is modified by the presence of electrolytes dissolved in the surrounding medium because the response of mobile ions in solution is to screen the electrostatic interaction between the two original charges (Harned and Owen, 1950). This effect can be treated by the Debye–Hückel model, which approximates the interaction energy of the two charges as (Hiemenz, 1977),

$$E_{q,q'} \cong \frac{qq'}{4\pi\epsilon}\frac{1}{|\mathbf{r} - \mathbf{r}'|}\exp(-\kappa|\mathbf{r} - \mathbf{r}'|), \tag{4}$$

where the previous interaction is now exponentially attenuated according to a screening distance parameter κ^{-1} that is a function of the solution ionic strength $I(\kappa \propto I^{1/2})$. This expression is applied to the interaction of the edge charges on a helically wound bilayer ribbon by introducing a line distribution of charge λ. The interaction energy assumes an integral form,

$$E_{\lambda,\lambda'} \cong \frac{\lambda\lambda'}{4\pi}\int_{\lambda edge} dl \int_{\lambda' edge} \frac{\exp(-\kappa|\mathbf{r} - \mathbf{r}'|)}{\epsilon(\mathbf{r}, \mathbf{r}')|\mathbf{r} - \mathbf{r}'|} dl' \tag{5}$$

in which the double integration is taken over increments dl and dl' along the two respective edges so as to incorporate all pair interactions of charge between the two edges. The dielectric response $\epsilon(\mathbf{r}, \mathbf{r}')$ is now included within the integrations to account for the polarization effects from the bilayer as well as the surrounding medium. This distinction may be neglected, though, because the predominant interactions for a helical conformation of significant curvature ($P < L$) are mediated through the surrounding phase. The interaction energy is then reasonably well approximated by employing the dielectric constant of the surrounding medium, thereby simplifying the numerical evaluation of the integrations (Chappell and Yager, 1991*a*).

The edge charges on the bilayer ribbon derive from an electric dipole that will symmetrically place opposite charges on opposing edges of the ribbon. The total energy due to charge interactions involves all charge pair interactions that exist for the two oppositely charged edges. These interactions not only entail all pair-wise interactions between the two oppositely charged edges, but also those interactions among the like charges along each of the two respective edges. Hence, the total energy due to electrostatic interaction is,

$$E_{elec} = E_{+,-} + \tfrac{1}{2}(E_{+,+} + E_{-,-}), \tag{6}$$

where the energy terms are designated according to the sign of the charge on the interacting edges. These individual terms are each given by the electrostatic interaction energy formulated in Eq. 5, which inadvertently sums the pair-wise interactions twice for the self-interaction energy of an edge, requiring the inclusion of a one-half factor.

The potential energy from the electrostatic interactions that actually induce the ribbon to curl is given by the difference between the helically wound and flat configurations of the bilayer ribbon,

$$\Delta E_{elec}(a) = E_{elec}(a) - E_{elec}(\infty), \tag{7}$$

where the curvature of the bilayer is designated by the radius a of the helical conformation under consideration. The total potential energy associated with the curvature of the bilayer ribbon is thus finally described by the two opposing energy contributions,

$$\Delta E_{cur}(a) = \Delta E_{elec}(a) + \Delta E_{strain}(a) \tag{8}$$

in which the positive contribution from the elastic strain must be compensated by the electrostatic interactions if curvature is to become spontaneous. The elastic strain from curvature assumes the conventional form (Helfrich, 1986),

$$\Delta E_{strain}(a) = \frac{1}{2}K\frac{A}{a^2} \tag{9}$$

in which A is the area of the ribbon and K is the elastic modulus appropriate for bending the bilayer about its preferred axis of curvature.

Application to bilayer microstructures

The results of this treatment for a bilayer ribbon of standard dimensions ($L = 70$ μm and $\delta = 3.1$ μm) yields the potential energy profiles for curvature in Fig. 2, as a function of the strength of electrolyte screening. The curves span a transition from a ribbon that spontaneously winds into a tubule of length $L = 70$ μm and radius $r = 0.5$ μm, to a ribbon that is blocked from curling by a potential energy barrier ΔE^*_{cur}. This barrier is due to the elastic stain from curvature, and develops as the electrostatic interactions that stabilize curvature become increasingly screened by greater concentrations of ions in solution. The profiles of Fig. 2 correspond to dilute levels of electrolytes, which range from the complete absence of dissolved ions ($I = 0$, $\kappa^{-1} \to \infty$), to a micromolar concentration ($I \sim 1$ μM, $\kappa^{-1} \sim 0.3$ μm), and above ($I > 100$ μM, $\kappa^{-1} < 0.03$ μm). Electrolyte effects on tubule formation can become pronounced as the screen-

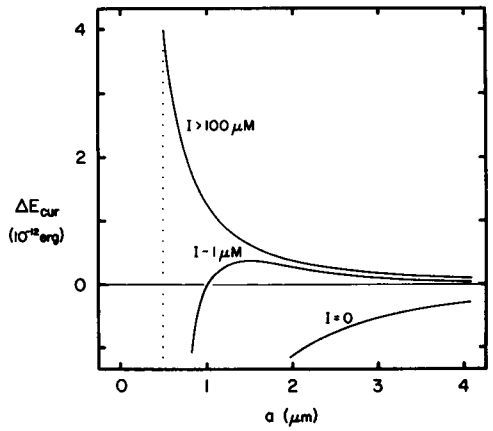

FIGURE 2 Potential energy profiles (ΔE_{cur} versus a) for the curvature of a helically-wound ribbon as a function of the solution ionic strength (I) due to electrolytes dissolved in the surrounding aqueous medium. The profiles apply to a bilayer ribbon of appropriate dimensions (L = 70 μm, δ = 3.1 μm) with a polarization charge density (λ = 0.0002 esu/cm) adequate to stabilize the curvature of a bilayer with low rigidity ($K = 1.0 \times 10^{-14}$ erg) into a tubule of typical dimensions (L = 70 μm, r = 0.50 μm) in dilute electrolytes. The dotted vertical line indicates the radius at which the helically-wound ribbon forms a tubule.

ing distance approaches the diameter of the prospective tubule and the potential barrier becomes too great for thermal activation (10 kT ~ 4×10^{-13} erg). The profile $I \sim 1$ μM of Fig. 2 depicts this threshold region, where electrolyte screening becomes critical and the potential barrier can block tubule formation. Tubules of $DC_{8,9}PC$, with diameters near 1 μm, are then likely to be inhibited from forming at electrolyte levels above a micromolar concentration if electrostatic interactions stabilize their curvature. The rigidity of the bilayer largely determines the height of the barrier, and for a distinctly large polarization charge density (λ ~ 0.0002 esu/cm) along the bilayer edges,[1] the elastic modulus for bending must be relatively small ($K \sim 10^{-14}$ erg) if curvature of the bilayer into a tubule is to occur. A greater rigidity is in fact expected for a solidus bilayer ($K > 10^{-12}$ erg) (Helfrich, 1986), which would block tubule formation entirely, even in the absence of any electrolyte. So a relatively small bending modulus appears to be a prerequisite if electrostatic interactions are to be sufficient to stabilize the curvature of a bilayer into a one micron diameter tubule. However, a low modulus bilayer remains extremely sensitive to the electrolyte level, and a modest increase to a millimolar concentration ($I \sim 1$ mM, $\kappa^{-1} \sim 0.01$ μm) should thoroughly screen any electrostatic interactions and leave a prohibitive barrier ($\Delta E^*_{cur} \sim 100$ kT) to be scaled for tubule formation.

A change in the dimensions of the bilayer ribbon may alter the potential energy profile for curvature because this alters the magnitude of both the electrostatic interaction as well as the elastic strain incurred by the bilayer with curvature. The length of the ribbon determines the amount of charge involved in the electrostatic interaction, and the ribbon width is instrumental in establishing the distances over which the charge interactions occur for a given curvature. The ribbon width also determines the diameter of the prospective tubule and thereby dictates the magnitude of the elastic strain. The potential energy profile for curvature is then highly dependent upon the length to width ratio of the ribbon (aspect ratio L/δ), as well as the overall size of the ribbon (area A). Consequently, tubule formation may be determined by the growth pattern of the bilayer. Specifically, a reduction in the aspect ratio of the ribbon could improve the prospects for curvature because this directly lowers the total elastic strain for bending the bilayer by either decreasing the curvature of the ribbon or by reducing the total ribbon area. However, if growth in the bilayer produces a proportional increase in both the ribbon width and length (L/δ is constant), the potential barrier due to the elastic strain from curvature is unaffected by any change in the ribbon size.

The effect of the electrostatic interaction on the potential barrier as a function of ribbon size is shown in Table 1. In the limit of small ribbons, the electrostatic interaction is vanishingly small since the electrostatic interaction energy is proportional to the amount of edge charge, and thereby the length of the ribbon (Chappell and Yager, 1991*a*).

Consequently, this interaction proportionally increases in strength with the ribbon size and in the

TABLE 1 Potential energy barrier to curvature as a function of the solution ionic strength for several magnitudes of bilayer ribbon size

Ribbon size‡	$\Delta E^*_{cur}(kT)$		
	$I = 0$	$I \sim 1$ μM	$I > 100$ μM
0.01	100	100	100
0.1	34	35	100
1	0	7	100
10	0	60	100
100	0	100	100

Potential energy barrier (ΔE^*_{cur}) is defined as the maximum positive value of the potential energy profile for curvature and is evaluated for the bilayer properties cited in Fig. 2. Values are expressed in units of kT at room temperature (300 K ~ 4×10^{-14} erg).

‡The size parameter scales the dimensions of a bilayer ribbon of a standard size (L = 70 μm and δ = 3.1 μm).

[1]This implies a very large dipole contribution (~0.5 D) from each molecule (de Gennes, 1987).

absence of electrolyte erodes the potential barrier to stabilize curvature for ribbons larger than a given size. This behavior is profoundly changed when electrolyte screening is introduced, as seen in Table 1 for a micromolar presence of ions. Now an increase in ribbon size no longer progressively improves the profile for curvature and the potential barrier ultimately returns to its maximum height for large ribbons. This is the consequence of electrolyte screening becoming more thorough for interactions over greater distances, particularly when the screening distance becomes significantly less than the radius of the prospective tubule. For higher levels of electrolytes, the screening distance continues to decrease and the electrostatic interaction becomes increasingly ineffective for smaller ribbon sizes. This trend proceeds to weaken the electrostatic interaction to a point at which tubule formation is inhibited for any ribbon size. Electrolyte levels in excess of 100 μM effectively eliminate the electrostatic interaction, and the potential energy barrier to curvature attains its maximum height for all ribbon sizes (Table 1).

Bilayer tubule formation is therefore expected to be extremely sensitive to low levels of electrolyte if an electrostatic interaction is responsible for stabilizing the curvature of the bilayer. Destabilization of bilayer curvature by electrolytes, however, may not simply block tubule formation since the curvature of ribbons with a lower aspect ratio may be thermally activated to produce a tubule. A decrease in the aspect ratio of the bilayer ribbon will lower the barrier to curvature, as demonstrated by the potential energy profiles in Fig. 3 for a progressive increase in the ribbon width. A sufficient decrease in the aspect ratio may then allow for thermal excitation over the barrier to produce a tubule, and an alternative response to an increased concentration of electrolyte could be the formation of either shorter and/or larger diameter tubules. The profiles of Fig. 3 show that an order of magnitude decrease in the aspect ratio may reduce the barrier adequately for thermal activation. The mechanisms of bilayer growth must then enable this appropriately proportioned ribbon to develop, otherwise, the elastic strain for the curvature of the bilayer ribbon will remain excessive and the effect by electrolyte to destabilize bilayer curvature will prevent tubule formation. A general effect by dissolved electrolytes to profoundly decrease the aspect ratio or prevent the formation of $DC_{8,9}PC$ tubules is therefore predicted if an electrostatic interaction stabilizes the curvature of these microstructures to any significant degree.

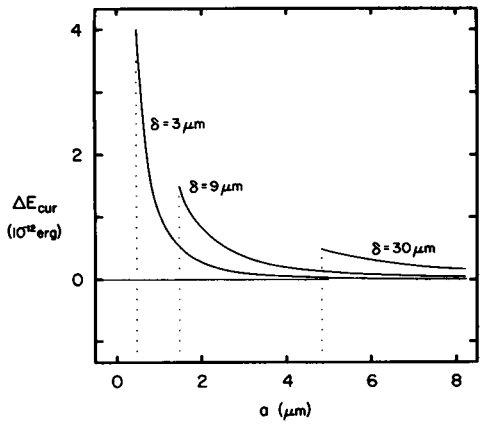

FIGURE 3 Potential energy profiles (ΔE_{cur} versus a) for the curvature of a helically-wound ribbon in the absence of an electrostatic interaction to stabilize curvature, as a function of the ribbon width (δ). The profiles concern ribbons with the same length (L = 70 μm) and the same bilayer properties as for Fig. 2.

MATERIALS AND METHODS

The diacetylenic phospholipid $DC_{8,9}PC$ was obtained from Avanti Polar Lipids, Inc. (Birmingham, AL) in reasonably high purity, and gave a single spot by thin layer chromatography on silica gel plates. The method used to prepare the tubular microstructures (and investigate the effects from electrolytes) was based on the precipitation of the lipid from ethanolic solutions upon the addition of water (Georger et al., 1987). Ethanolic solutions of $DC_{8,9}PC$ (0.2–1.0 mg/ml) were rapidly mixed with deionized/distilled water to produce reaction solutions (30–50% water by volume) at room temperature (21 ± 1°C). Precipitation occurred within a few seconds of mixing as evident from the development of a white and slightly opalescent turbidity.

Studies on the effect of electrolytes were conducted for a variety of inorganic salts at concentrations ranging from 1.0 mM to 1.0 M. The salts were selected to be either sodium or chloride containing electrolytes in order to examine the effects of different cationic species in the presence of a common anion (HCl, LiCl, NaCl, KCl, NH_4Cl, $MgCl_2$, $CaCl_2$, $AlCl_3$, $FeCl_3$), as well as different anionic species in the presence of a common cation (NaOH, NaF, NaCl, NaBr, NaI, $NaNO_3$, $NaHCO_3$, Na_2HPO_4, Na_2SO_4). All electrolytes were analytical or reagent grade chemicals, and absolute ethanol of reagent quality was used for all experiments. Control experiments employed deionized/distilled water with a large specific resistivity (10^7 Ω-cm) that corresponds to a background concentration of ions less than 10 μM. Electrolyte effects on $DC_{8,9}PC$ tubule formation were generally performed with the electrolyte dissolved in the aqueous solution before mixing with the ethanolic solution of lipid. This was due to the limited solubility of the salts in ethanol, although studies observing effects of millimolar electrolyte also considered the electrolyte dissolved with the lipid in ethanol prior to the addition of water. The final composition of the reaction solutions were commonly near 70% ethanol/30% water by volume, with the exception of studies at 1.0 M electrolyte, where a 50% ethanol/50% water composition was used to improve the solubility of some salts. This difference in composition of the reaction solution had negligible effects on tubule precipitation as apparent from control studies. Several salts (NaF, $NaHCO_3$, Na_2HPO_4, Na_2SO_4, and KCl) however, remained largely insoluble at high concentrations, so their molar presence during lipid precipitation could not be explored. The effects from 1.0 M HCl and NaOH were also not forthcoming due to the rapid hydrolysis of lipid under these extremes

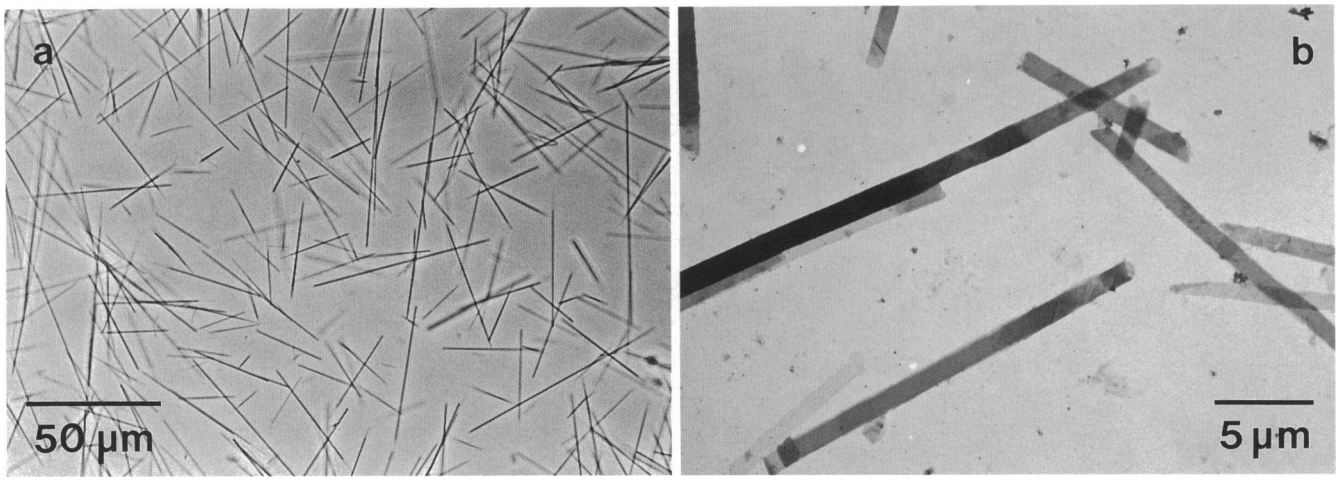

FIGURE 4 Micrographs of tubular microstructures precipitated from ethanol solutions of $DC_{8,9}PC$ upon the addition of deionized/distilled water. Optical micrograph (*a*) of tubules dispersed in the reaction solution. Transmission electron micrograph (*b*) of tubules dried onto a formvar-coated grid.

in solution pH. Most experiments were performed in solutions near neutral pH (5–8), although a few salts required a lower pH (2–4) to prevent precipitation of the metal hydroxide ($AlCl_3$, $FeCl_3$) or higher pH (8–10) to stabilize the anionic specie ($NaHCO_3$, Na_2HPO_4).

Effects on tubule formation were primarily monitored by phase contrast optical microscopy, employing a Zeiss inverted microscope (model ICM 405; Carl Zeiss Inc., Thornwood, NY). The microstructures precipitated from the reaction solutions were observed directly from droplets of the reaction solution placed on a glass slide and compressed with a cover slip. The first microscope observations were made within 24 h of the initial mixing of solutions, and only minor variations in the appearance or size distribution of the microstructures occurred over the following 3–4 wk. These optical observations were supplemented by transmission electron microscopy using a Jeol transmission electron microscope (model 1200; Jeol Instruments Inc., Peabody, MA). Samples were prepared by air drying a droplet of the reaction solution on a formvar-coated copper grid.

Calorimetry studies were performed using a Seiko Instruments differential scanning calorimeter (model DSC 100; Seiko Instruments U.S.A. Inc., Torrance, CA) as an additional means to detect electrolyte effects on the relative stability of the crystalline bilayer state of the $DC_{8,9}PC$ tubules. These structures when dispersed in water characteristically display a chain melting transition to a liquidus bilayer at the reported temperature of 43.2°C (Yager and Schoen, 1984) with an enthalpy of 23.0 kcal/mol (Singh et al., 1988). Calorimetry was conducted on both microstructures precipitated in the presence of electrolyte, as well as on tubules prepared under control conditions and then presented with electrolyte. Calorimetry measurements were preferably made on precipitates dispersed in purely aqueous environments since aqueous dispersions were desirable as a standard environment that is more readily reproduced than ethanol/water solutions.[2] This required all precipitates to be separated from their reaction solutions by centrifugation (~8,000 *g* for 10 min) and then washed once and redispersed in aqueous solutions with the relevant electrolyte concentration. The microstructures showed no visible effects from this treatment and displayed the same physical characteristics in an aqueous dispersion as evident by optical microscopy. These dispersions were centrifugated once again and the solution phase was reduced so as to concentrate the dispersion to near 10 mg of lipid per mL. Calorimetry was performed on 50 μl samples of the concentrated dispersions versus a 50 μl reference of the aqueous solution or water. All measurements were conducted under the same instrument conditions (heating rate of 0.2°C per min), and the results for transition temperatures were highly reproducible (±0.1°C). Enthalpy values for the transition did show some variability (22 ± 2 kcal/mol), presumably due to limitations in the quantitative manipulation of the small dispersion samples.

[2]Calorimetry studies on samples dispersed in ethanol/water solutions display an analogous chain melting transition to that in aqueous solutions with the exception of a depressed transition temperature that is dependent upon the fraction of ethanol in the solution phase.

RESULTS

Microscopy observations

The precipitation of $DC_{8,9}PC$ lipid in the absence of any added electrolytes produced tubular microstructures in accordance with previous studies (Georger et al., 1987), and with the typical appearance displayed in Fig. 4. Helically wound ribbons of bilayer were not as readily apparent, although they are often difficult to distinguish from the tubular forms by optical microscopy. The dimensions of the bilayer tubules fall within a wide range of lengths (20–200 μm), but with fairly similar diameters (0.8 ± 0.2 μm). Electron microscopy reveals the multilamellar nature of these microstructures, as well as a helical substructure suggested by striations in some regions of the bilayer (Fig. 4 *b*). The origin of this last feature is not known, although the striations may reveal

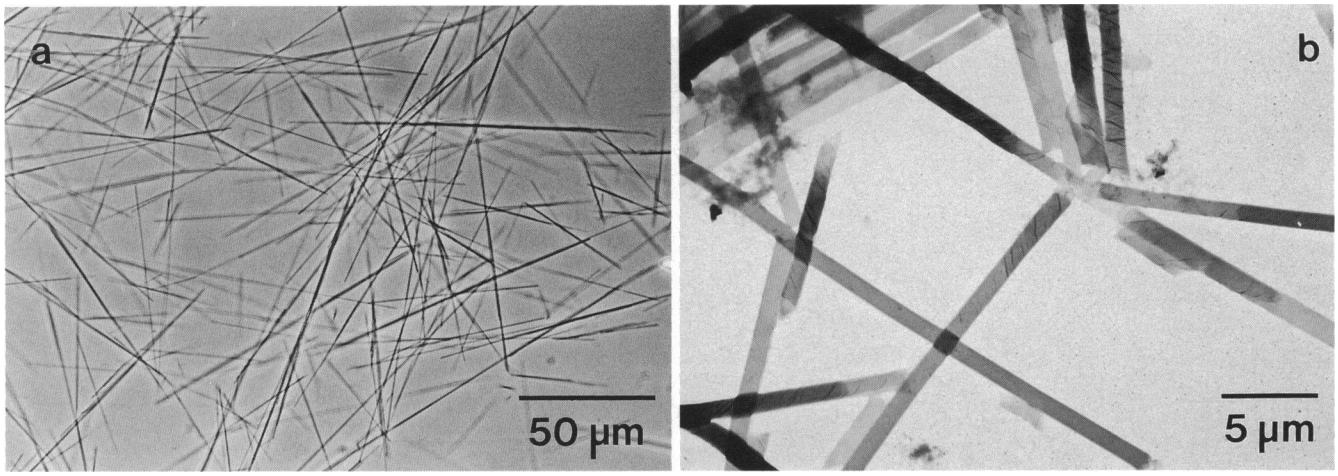

FIGURE 5 Micrographs of tubular microstructures precipitated from ethanol solutions of $DC_{8,9}PC$ in the presence of 1.0 mM NaCl. Optical (*a*) and electron (*b*) micrographs of tubules show no difference in appearance from that prepared under control conditions.

a linear association to the molecular packing within the plane of the bilayer (Chappell and Yager, 1991*b*).[3]

When a millimolar level of electrolyte is present prior to precipitation, no profound effect is made on tubule formation and the precipitation phenomenon appears visually the same as with the control. This was the case for either means of electrolyte addition: whether the electrolyte was present with the lipid in the ethanolic solution prior to water addition, or the electrolyte was introduced as a part of the aqueous solution. The microstructures prepared in 1.0 mM NaCl are shown in Fig. 5 and appear indistinguishable in their physical characteristics from the control structures in Fig. 4. The substructure (Fig. 5 *b*) displays the same helical striations and dimensions as that of the tubules produced in the absence of added electrolyte (Fig. 4 *b*). This observation is essentially the same for all of the sodium salts employed in this survey, regardless of anionic species. Similarly, no discernable effect is evident with the chloride salts of the other monovalent cations (LiCl, KCl), as well as the divalent cations ($MgCl_2$, $CaCl_2$). The trivalent cations ($AlCl_3$, $FeCl_3$) are the only electrolyte species found in this survey to perturb the dimensions of the tubular microstructures at this concentration. The curvature of the bilayer appears unaltered but the lengths of these tubules, as revealed in Fig. 6, are considerably shortened by 1.0 mM of Fe^{3+} and Al^{3+} in acidic reaction solutions (pH 2 and 4, respectively). The low pH that is necessary for the solubility of the cation species is not in itself responsible for the restriction in tubule length because typical structures develop in moderately acidic solutions.

Increasing the concentration of these electrolytes has little added effect on precipitation and the appearance of the $DC_{8,9}PC$ tubules until the molar level is attained. The precipitation phenomenon then appears to involve flocculation, as the turbidity is no longer homogeneously dispersed throughout the reaction solution, but discrete clumps of precipitate become visually discernable. The monovalent and divalent cation salts at this concentration do not inhibit tubule formation, though they do noticeably modify the appearance of the microstructures as illustrated in Fig. 7. All of the monovalent cation electrolytes produce tubules that are typified by those in 1.0 M NaCl (Fig. 7 *a*). These tubules can display a slightly larger outer diameter (1.0–1.5 μm) over that of the control (<1.0 μm) with a somewhat irregular surface that may suggest the attachment of additional bilayers to the main tubular structure. The outer diameter can increase further (1.0–2.0 μm) for the microstructures prepared in 1.0 M $MgCl_2$ (Fig. 7 *b*) as both the lumen diameter and tubule wall thickness of these tubular structures may possibly increase. This effect is also established in preparations in 1.0 M $CaCl_2$ (Fig. 7 *c*) as most of the tubules possess diameters greater than that of the control (Fig. 4 *a*). The bright halo observed around many of the tubules is an artifact associated with the phase contrast imaging of a strong phase object, and indicates a change in the optical properties and/or an increase in the diameter of the tubular structures (Pluta, 1989). These unusual microstructures also display a pronounced optical birefringence of the tubule walls that is not observed for any other $DC_{8,9}PC$ lipid struc-

[3]The striations may arise as an artifact due to drying or electron irradiation of the tubules (Yager et al., 1985).

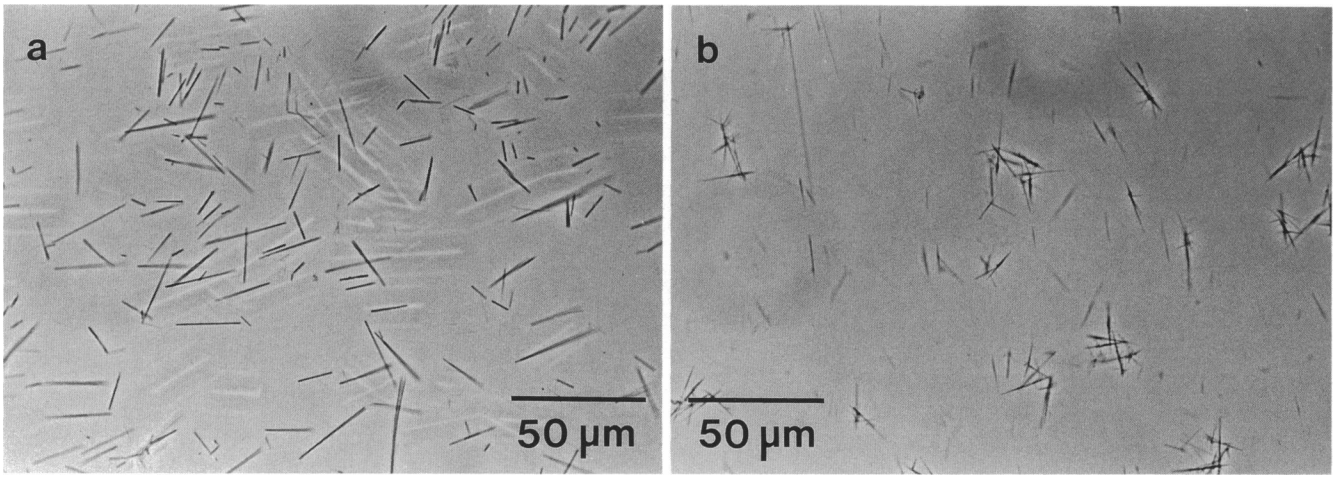

FIGURE 6 Optical micrographs of tubular microstructures precipitated from ethanol solutions of $DC_{8,9}PC$ in the presence of 1.0 mM trivalent cation salts at low pH. Micrographs (*a*) of shortened tubules prepared in $FeCl_3$ solution (pH ~2). Micrograph *b* of similar microstructures prepared in $AlCl_3$ solution (pH ~4).

tures prepared in the presence of other electrolytes. This observation, made upon viewing the specimen through crossed polarizers, is shown in Fig. 7 *d*. The lumen can be resolved between the tubule walls for many of the images, and the dimensions of these features suggest that the tubule walls may indeed be thicker (several tenths of a micron) for many of the tubular microstructures prepared in divalent cation salts.

The greatest effect observed on the formation of $DC_{8,9}PC$ tubules is that produced in the presence of 1.0 M $AlCl_3$, where distinct tubular structures are no longer apparent, but aggregates of spheroidal microstructures are the result, as shown in Fig. 8. The individual spheroidal forms appear to possess a radially organized substructure, and close examination of the irregular periphery does reveal some elongated features projecting out from the structures (Fig. 8 *b*). These needle-like projections may be tubular in form, although the existence of small bilayer helices or tubules could not be confirmed by microscopy. The spheroidal structures fail to show any optical birefringence and are too thick to reveal any substructure by transmission electron microscopy. Similar observations for high levels of other trivalent cationic species (i.e., Fe^{3+}) are not possible due to the extreme conditions required (pH < 1) for an increased solubility of these ions.

Calorimetry results

All of the microstructures prepared in this survey produce an endothermic peak in the DSC signal of very similar enthalpy and onset temperature as that expected for the chain melting transition of $DC_{8,9}PC$ tubules. The enthalpy observed for the transition of all structures fell within a range (22 ± 2 kcal/mol)[4] consistent with the value reported for $DC_{8,9}PC$ tubules prepared in the absence of added electrolyte (23.0 kcal/mol) (Singh et al., 1988). Similarly, the results for the tubules prepared before a millimolar concentration of the salts showed insignificant variations on the transition temperature (43.5 ± 0.1°C). Higher levels of some electrolytes, however, do influence the transition weakly, as illustrated by the transition temperatures listed in Tables 2 and 3 for the microstructures produced in the presence of 1.0 M electrolyte. Interestingly, the transition temperature T_m^* for the microstructures prepared in the presence of an electrolyte does not vary appreciably from the transition temperature T_m for tubules prepared under control conditions and subsequently introduced to the same electrolyte. This is particularly notable for the birefringent tubules and the non-tubular structures, suggesting that these forms are composed of a very similar crystalline bilayer state as in typical $DC_{8,9}PC$ tubules. The presence of electrolyte appears only to weakly perturb the transition of the crystalline bilayer to the liquidus state, as all of the bilayer forms are observed to convert into a liposome morphology above the transition temper-

[4]One exception was observed with the precipitation of lipid in 1.0 mM NaOH (T_m^* ~ 42°C), where only a small enthalpy change is observed for the chain melting transition, but the dilute appearance of the dispersion of tubules suggests considerable decomposition of the lipid (apparently due to hydrolysis of the head group).

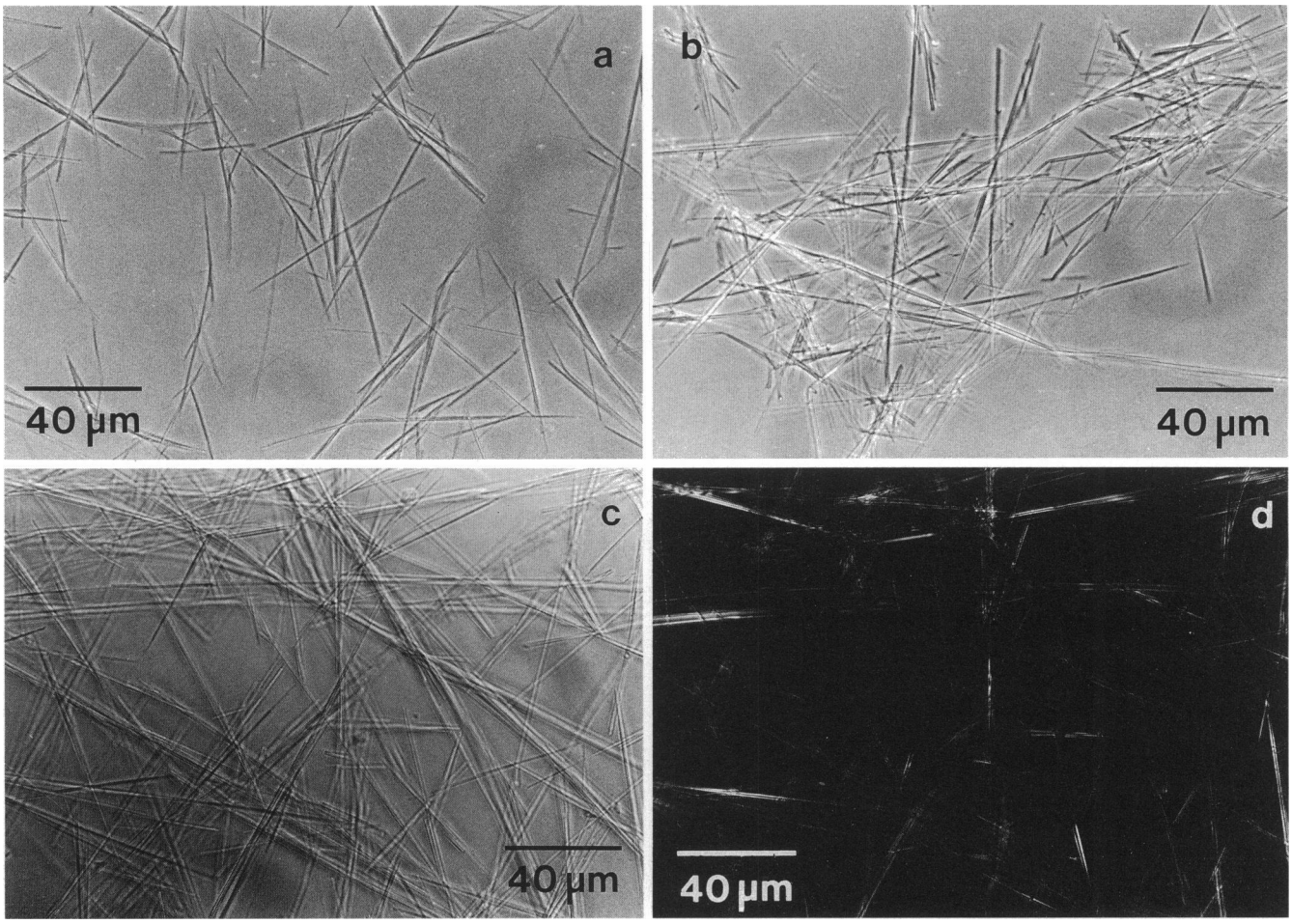

FIGURE 7 Optical micrographs of tubular microstructures precipitated from ethanolic solutions of $DC_{8,9}PC$ in the presence of 1.0 M monovalent and divalent cation salts. Micrographs *a*, *b*, and *c* of modified tubular microstructures prepared in solutions of NaCl, $MgCl_2$, and $CaCl_2$, respectively. Micrograph *d* of the same field in *c* as viewed through crossed polarizers. This image reveals optical birefringence of the tubule walls for many of the microstructures.

ature. A small increase in the transition temperature is the general result, with the divalent and trivalent cationic species providing the most pronounced shifts in T_m. The one exception is the decrease produced by NaI, which appears analogous to the chain melting point depression produced by iodide ion on other phosphatidylcholine bilayer systems (Simon et al., 1975).

DISCUSSION

Comparisons to theory

The appearance of a stable cylindrical curvature for the microstructures in Figs. 5 and 6 demonstrates the lack of any general effect by electrolytes at millimolar concentration to interrupt the forces stabilizing curvature in $DC_{8,9}PC$ tubules. The diameter appears unaltered in all of these structures, and thus no significant change in the degree of curvature is effected. The only noticeable change in morphology is a general reduction in the length of the tubules prepared in the presence of trivalent cations (Fig. 6). Most of these tubules fall within a range of short lengths (25 ± 10 μm), and are approximately one third the average length (~75 μm) observed for standard populations of $DC_{8,9}PC$ tubules.

This description does not agree with the predictions of theory for the stabilization of bilayer curvature by the electrostatic interaction of edge charges. The trivalent cationic species do produce shortened tubules of similar diameter, although the change in length appears insufficient to adequately reduce the elastic strain and allow curvature of the bilayer by thermal activation. Increased

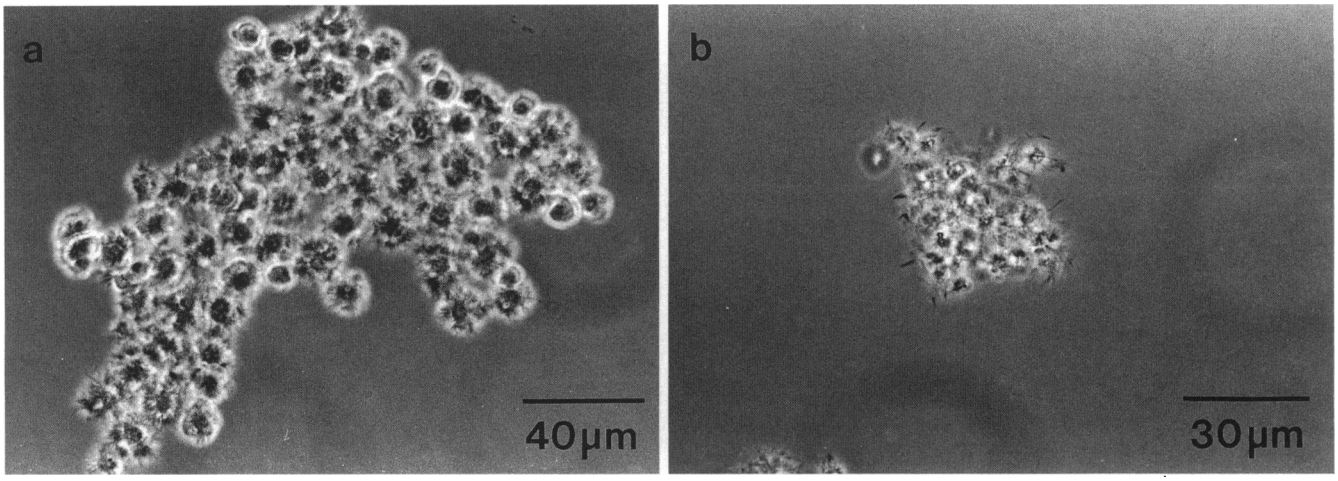

FIGURE 8 Optical micrographs *a* and *b* of spheroidal structures precipitated in the presence of 1.0 M $AlCl_3$. Micrograph *b* shows elongated features that may be tubular in form projecting out from the edge of some of the structures.

levels of electrolyte also fail to produce any general action to block tubule formation, as tubular microstructures continue to form in the presence of most electrolytes at molar concentrations. The only case in which the distinctive tubular forms are absent occurs with the precipitation of lipid in 1.0 M $AlCl_3$. The absence of any comparable effect by other dissolved salts argues that this phenomenon is specific to Al^{3+} (and perhaps other trivalent cations) and is not a general electrolyte effect.

The limited effects by dissolved electrolytes dismiss the viability of an electrostatic interaction as the means by which curvature is stabilized in $DC_{8,9}PC$ tubules, although the observations remain quite compatible with an intrinsic curvature for the bilayer as proposed in alternative theories (Helfrich, 1986; Helfrich and Prost, 1988; Yager et al., 1991). An intrinsic curvature, which becomes stable for some packing states of the bilayer, can account for the relatively similar diameter observed among the $DC_{8,9}PC$ tubular structures so long as the molecular packing within the tubular bilayer is not significantly affected by ionic interactions with dissolved electrolytes. Presumably, the crystalline packing of this bilayer state is not very dependent on polar or ionic interactions among the head groups, which are likely to be influenced by dissolved electrolytes. Cationic interactions with phosphatidylcholine bilayers can affect the conformation of the phosphocholine moiety, but no structural changes are detected in either the glycerol backbone nor the beginning of the fatty acyl chains (Akutsu and Seelig, 1981). The stability of the crystalline state for the $DC_{8,9}PC$ bilayer may then principally derive from interactions within the hydrophobic region of the bilayer and may not be very sensitive to interactions from ionic species in the aqueous phase. The calorimetry results agree with this description because minimal effects are made to influence the stability of the tubular crystalline state relative to the liquidus state of the bilayer. The transition temperature for chain melting within the $DC_{8,9}PC$ tubules is totally unaffected by a millimolar concentration of ions, and only relatively small increases in T_m occur at molar levels (Tables 2 and 3). These effects are comparable with, if not less than, those made by electrolytes on the main chain melting transition of other phosphatidylcholine bilayers (Simon et al., 1975; Chapman et al., 1977; Cunningham et al., 1986), in which the phase transition is strictly attributed to melting the hydrophobic core of the bilayer (Bartucci et al., 1990). These observations are consistent with the concept that the crystalline state of $DC_{8,9}PC$ tubules predominantly derives from packing interactions within the hydrophobic region of the bilayer. Notably, the other most significant effect by an electrolyte is the depression of the transition temperature by NaI, in which the iodide ion apparently produces a chaotropic effect through some weak hydrophobic interaction with the bilayer (Hatefi and Hanstein, 1969; Simon et al., 1975).

The crystalline packing of the $DC_{8,9}PC$ tubules apparently develops in the presence of electrolyte despite alterations in the resultant microstructure. The shortened tubules prepared in 1.0 M $AlCl_3$ and $FeCl_3$ (Fig. 6) show no difference in transition temperature from that of the tubules formed under control conditions or in millimolar levels of other electrolytes. Similarly, the modified structures precipitated in a molar concentration of electrolytes display transition temperatures comparable to that of tubules prepared under control conditions and then introduced to the electrolyte. This is especially noteworthy for the microstructures prepared

TABLE 2 **Onset temperature of chain melting transition for $DC_{8,9}PC$ microstructures in the presence of chloride salts at molar levels.**

Salt	T_m^*(°C)‡§	T_m(°C)‡
Control	43.4 [0.3]	43.4 [0.3]
1.0 M LiCl	44.4 [0.3]	44.4 [0.3]
1.0 M NaCl	43.7 [0.3]	43.5 [0.3]
1.0 M KCl	---	44.0 [0.3]
1.0 M NH_4Cl	44.1 [0.3]	44.1 [0.3]
0.5 M $MgCl_2$	···	44.5 [0.3]
1.0 M $MgCl_2$	44.6 [0.2]	44.8 [0.3]
0.5 M $CaCl_2$	···	45.3 [0.3]
1.0 M $CaCl_2$	45.8 [0.3]	46.0 [0.3]
0.3 M $AlCl_3$	···	45.2 [1.5]
1.0 M $AlCl_3$	46.2 [1.0]	46.7 [1.2]

The onset temperature is defined by the point at which the tangent of the DSC signal with the greatest negative slope intersects the baseline of the signal trace (uncertainty ± 0.1°C).
*Transition temperature (T_m^*) of $DC_{8,9}PC$ microstructures precipitated in presence of the chloride salt, as opposed to the transition temperature (T_m) of $DC_{8,9}PC$ tubules prepared in the absence of added electrolyte and subsequently introduced to the chloride salt.
‡Bracketed value is the temperature width at half height of the melting endotherm peak in the DSC signal trace.
§No result due to salt insolubility (---) or to absence of experiment(···).

TABLE 3. **Onset temperature of chain melting transition for $DC_{8,9}PC$ microstructures in the presence of sodium salts at molar levels.**

Salt	T_m^*(°C)‡§	T_m(°C)‡§
Control	43.4 [0.3]	43.4 [0.3]
1.0 M NaF	—	44.2 [0.3]
1.0 M NaCl	43.7 [0.3]	43.5 [0.3]
1.0 M NaBr	43.6 [0.2]	43.6 [0.2]
1.0 M NaI	41.7 [0.3]	41.9 [0.3]
1.0 M $NaNO_3$	43.4 [0.3]	43.5 [0.3]
1.0 M $NaHCO_3$	—	44.1 [0.3]
0.5 M Na_2HPO_4	—	44.0 [0.3]
1.0 M Na_2HPO_4	—	—
0.5 M Na_2SO_4	—	44.0 [0.2]
1.0 M Na_2SO_4	—	44.6 [0.3]

The onset temperature is defined by the point at which the tangent of the DSC signal with the greatest negative slope intersects the baseline of the signal trace (uncertainty ± 0.1°C).
*Transition temperature (T_m^*) of $DC_{8,9}PC$ microstructures precipitated in the presence of the sodium salt, as opposed to the transition temperature (T_m) of $DC_{8,9}PC$ tubules prepared in the absence of added electrolyte and subsequently introduced to the sodium salt.
‡Bracketed value is the temperature width at half height of the melting endotherm peak in the DSC signal trace.
§No result due to salt insolubility (—).

in 1.0 M $AlCl_3$ (Fig. 8) because this precipitate has largely lost the tubular morphology. Apparently, all of the lipid structures consist of essentially the same crystalline bilayer state as characterized by a chain melting transition of similar onset temperature and enthalpy. The effect of some dissolved salts to modify, and in one case to destroy the tubular morphology, is then not from an appreciable change in the molecular packing of the bilayer state, but is apparently the result of changes in the size and arrangement of the domains of the $DC_{8,9}PC$ crystalline bilayer. The effects from electrolytes therefore appear to be kinetic, whereby the pattern of nucleation and growth of the crystalline bilayer is altered during precipitation.

Effects from monovalent and divalent cations

A trend to increase the outer diameter of the tubular bilayers by molar levels of monovalent and divalent cationic electrolytes is evident in Fig. 7 as the micrographs are viewed in sequence. The increase in outer diameter of these structures appears to arise from a thickening of the tubule wall, possibly as a result of additional bilayers depositing onto a preexisting tubule. Typical tubules of $DC_{8,9}PC$ are recognized to be multilamellar structures with the bilayer number varying from as few as one or two to as many as five or six (Yager et al., 1985). This corresponds to wall thickness of 5–30 nm. The walls of tubules prepared in divalent cations can be much thicker, as the images of the birefringent walls (Figs. 7 *d*) reveal some thicknesses to be greater than the resolution limit of optical microscopy (~ 0.4 μm).

The multilamellar substructure to $DC_{8,9}PC$ tubules is suggestive that the surface of a preexisting tubular bilayer serves as a site for new crystalline bilayers to nucleate and align, so with continued growth a bilayer is added over the original tubule. The curvature of successive layers deposited in this fashion will tend to decrease and deviate from a preferred equilibrium value, limiting further growth in tubule wall thickness. The resulting multilamellar tubule is then composed of concentric crystalline bilayers, with thin hydration layers between the polar region of adjacent bilayers. The extent of hydration is not known, although a region can be identified to exist between bilayers in transmission electron micrographs of freeze-fractured replicas of $DC_{8,9}PC$ tubules (Yager et al., 1988).

At moderate concentrations of electrolytes (>10 mM), the adsorption of both cations and anions can occur within the polar region at the surface of a phosphatidylcholine bilayer (Tatulian, 1983; Cunningham et al., 1986). Generally, cationic species present stronger interactions with the phosphocholine moiety and can bind within the head group array to establish a

net positive charge on the bilayer surface (Inoko et al., 1975; Lis et al., 1981*a*; Cunningham et al., 1986). This binding of cations to the bilayer can also induce changes in the conformation of the phosphocholine moiety and reorganize the structure within the polar region at the bilayer surface (Akutsu and Seelig, 1981; Bartucci et al., 1990). The multivalent cations prove the most effective among electrolyte species at influencing the head group structure (Akutsu and Seelig, 1981), whereby proximate phosphate groups within the head group array may chelate divalent or trivalent cations to produce some bridging of the head groups (Shah and Schulman, 1965). The positive charge imparted by the binding of cations establishes an electrostatic repulsion that is observed to separate multilamellar bilayers for a variety of phosphatidylcholine lipids (Lis et al., 1981*b*). Higher concentrations of the electrolyte, however, can act to screen this repulsive interaction, and above ~0.5 M the separation of bilayers is observed to decrease to the hydration limit (~2 nm) that occurs in the absence of added electrolyte (Inoko et al., 1975). The flocculation phenomenon observed in the precipitation of tubular microstructures of $DC_{8,9}PC$ in molar electrolyte is certainly consistent with the absence of any long-range repulsion between bilayers, and may even suggest an attractive interaction (beyond the hydration limit) that does not operate in the absence or dilute presence of electrolyte. This effect, combined with a heightened degree of order to the polar region of $DC_{8,9}PC$ bilayers, may favor the nucleation of additional bilayers onto a preexisting tubule. Possibly, the structured polar region of phosphocholine groups and bound cations communicates more effectively the crystalline order of the bilayer packing and becomes an improved site for the nucleation of a new bilayer. The enhanced nucleation of bilayers onto a preexisting tubule is likely to increase the degree of bilayer lamination of the tubules and lead directly to a greater thickness for the tubule walls. The increased lamination of anisotropic crystalline bilayers would intensify the optical birefringence of a multilamellar tubule wall, an effect that should become distinctly visible by optical microscopy as the wall thickness approaches the limit of optical resolution (~0.4 μm). The structure imposed on the polar region through the binding of Mg^{2+} and Ca^{2+} may also contribute to the packing anisotropy (and hence optical birefringence) of the tubule walls, though the primary effect from binding these divalent cations is presumably the enhanced lamination of additional bilayers over a $DC_{8,9}PC$ tubule.

Effects from trivalent cations

An alteration in the nucleation and crystalline growth of the bilayer also appears consistent with the observations made on the structures produced in the presence of trivalent cations, albeit a dramatically different result from that of divalent cations. The shortened tubules formed in a millimolar concentration (Fig. 6) may be interpreted as single crystal bilayers that have not grown to the size of tubules prepared under control conditions. This is not to suggest that less lipid has precipitated into the crystalline bilayer state of a tubule because the enthalpy change is the same as that anticipated for an equivalent amount of $DC_{8,9}PC$ lipid organized into tubules under control conditions. The tubules are therefore smaller, but apparently more numerous. The trivalent cations may then enhance the formation of stable nuclei, but unlike divalent cations, suppress the growth of these crystalline bilayers to ordinary tubule dimensions.

This effect appears to progress in the presence of $AlCl_3$ as the concentration of the salt is raised. Above 1 mM, shorter tubular structures are more numerous and are commonly observed to be associated with, and possibly connected to other tubules (Fig. 6 *b*). This suggests a phenomenon where the crystalline growth of individual bilayers becomes discouraged and new nuclei form more readily, particularly by budding off of a small, but preexisting bilayer structure. Ultimately, polycrystalline aggregates may result, in which the individual bilayer structures may become so small that a tubular form cannot be recognized. This description is consistent with the observations made on the spheroidal microstructures that form in the presence of 1.0 M $AlCl_3$ (Fig. 8). Distinct tubular structures are no longer prevalent, although calorimetry indicates a transition very similar to the chain melting transition observed for the crystalline bilayer state of the tubules. This behavior is analogous to that of the lamellar phase produced when $DC_{8,9}PC$ liposomes (prepared above 45°C) are supercooled to 4°C (Rudolph and Burke, 1987). A comparable chain melting transition upon heating is observed as well, without any appearance of tubular structures. Rapid crystallization by supercooling can commonly result in polycrystalline solids with small crystallite domains, since multiple nucleation events are favored and individual crystals do not grow as large (Adamson, 1982). The domains of bilayer in this lamellar phase are presumably arranged quite differently than in the microstructures of Fig. 8, which may be oriented with some radial symmetry within the spheroidal form. The mechanism by which aluminum salts induce this effect is unknown, although complexation between Al^{3+} and soluble phosphatidylcholine lipid molecules prior to or during precipitation is likely to occur, which may then profoundly affect the assembly of the amphiphilic molecules into a crystalline bilayer.

CONCLUSION

A general effect by dissolved electrolytes to destabilize the cylindrical curvature of bilayer tubules prepared from the diacetylenic phospholipid $DC_{8,9}PC$ is not observed. Tubular microstructures continue to precipitate from ethanolic solutions in the presence of molar levels of many common inorganic salts. These observations are not consistent with the proposition that the curvature in the tubules results from an electrostatic interaction of polarization charges on the edges of a ferroelectric bilayer ribbon. Such an interaction is predicted to be strongly attenuated by dilute to moderate concentrations of dissolved electrolytes, effecting a dramatic decrease in the aspect ratio of the bilayer tubule or preventing curvature entirely. The absence of these effects indicates that curvature in the $DC_{8,9}PC$ tubules is stabilized by an alternative means and possibly arises from a bending force intrinsic to the anisotropic crystalline state of the molecular packing within the bilayer.

Significant alterations in the appearance or dimensions of the tubules do occur as specific effects on tubule formation by a few electrolytes. One effect by divalent cations is the formation of tubular structures with thickened tubule walls that show a pronounced optical birefringence. These microstructures may result from an increased lamination of multiple bilayers onto the tubules through some effect from cation binding to the phosphocholine moiety of the $DC_{8,9}PC$ bilayer. A trivalent cation, however, proves to be destructive to the tubular morphology at high concentrations, as the lipid precipitates into progressively shorter tubules at ionic concentrations above 1 mM. This effect leads to a nontubular morphology at molar levels, where the domains of the crystalline bilayer presumably shrink to dimensions that are no longer recognized to possess a tubular form.

These effects by electrolytes are apparently kinetic phenomena, since calorimetry indicates that the same bilayer state exists in the modified structures as in typical tubules produced under control conditions. The chain melting transition in the modified as well as normal structures is only weakly perturbed by a molar level of electrolyte. Consequently, the ionic interactions of dissolved electrolytes with the phosphocholine head groups of $DC_{8,9}PC$ do not appear to significantly influence the relative stability of the crystalline state of the bilayer tubule, but only its nucleation and growth when the lipid precipitates from solution. The stability of this state, and the origin of any intrinsic bending forces within the bilayer, appear then to largely derive from intermolecular packing interactions within the hydrophobic region of a $DC_{8,9}PC$ lipid bilayer.

The authors thank Dr. Marie Cantino for her expertise and assistance with transmission electron microscopy.

The authors also acknowledge support from the National Science Foundation through grant number CBT-8815027.

Received for publication 22 March 1991 and in final form 28 May 1991.

REFERENCES

Adamson, A. W. 1982. Physical Chemistry of Surfaces. Wiley, New York. 319–331.

Akutsu, H., and J. Seelig. 1981. Interaction of metal ions with phosphatidylcholine bilayer membranes. *Biochemistry* 20:7366–7373.

Archibald, D. D. 1990. Structural studies of high aspect-ratio self-assembled lipid microstructures with the use of microscopy and FT-NIR Raman spectroscopy. Ph. D. thesis, University of Washington, Seattle, WA.

Bartucci, R., N. Gulfo, and L. Sportelli. 1990. Effect of high electrolyte concentration on the phase transition behaviour of DPPC vesicles: a spin label study. *Biochim. Biophys. Acta.* 1025:117–121.

Chapman, D., W. E. Peel, B. Kingston, and T. H. Lylley. 1977. Lipid phase transitions in model biomembranes: the effect of ions on phosphatidylcholine bilayers. *Biochim. Biophys. Acta.* 464:260–275.

Chappell, J. S., and P. Yager. 1991*a*. Electrostatic interactions within helical structures of chiral lipid bilayers. *Chem. Phys.* 150:73–79.

Chappell, J. S., and P. Yager. 1991*b*. A model for crystalline order within helical and tubular structures of chiral bilayers. *Chem. Phys. Lipids.* 58:253–258.

Cunningham, B. A., J. E. Shimotake, W. Tamura-Lis, T. Mastran, W.-M. Kwok, J. W. Kauffman, and L. J. Lis. 1986. The influence of ion species on phosphatidylcholine bilayer structure and packing. *Chem. Phys. Lipids.* 39:135–143.

de Gennes, P. G. 1974. The Physics of Liquid Crystals. Clarendon, Oxford.

de Gennes, P. G. 1987. Electrostatic buckling of chiral lipid bilayers. *C. R. Acad. Sci. Paris.* 304:259–263.

Georger, J. H. A. Singh, R. R. Price, J. M. Schnur, P. Yager, and P. E. Schoen. 1987. Helical and tubular microstructures formed by polymerizable phosphatidylcholines. *J. Am. Chem. Soc.* 109:6169–6175.

Harned, H. S., and B. B. Owen. 1950. The Physical Chemistry of Electric Solutions. Reinhold, New York.

Hatefi, Y., and W. G. Hanstein. 1969. Solubilization of particulate proteins and nonelectrolytes by chaotropic agents. *Proc. Natl. Acad. Sci. USA.* 62:1129–1136.

Helfrich, W. 1986. Helical bilayer structures due to spontaneous torsion of the edges. *J. Chem. Phys.* 85:1085–1087.

Helfrich, W., and J. Prost. 1988. Intrinsic bending force in anisotropic membranes made of chiral molecules. *Phys. Rev.* A38:3065–3068.

Hiemenz, P. C. 1977. Principles of Colloid and Surface Chemistry. Marcel Dekker, New York. 352–391.

Inoko, Y., T. Yamaguchi, F. Furuya, and T. Mitsui. 1975. Effects of cations on dipalmitoyl phosphatidylcholine/cholesterol/water system. *Biochim. Biophys. Acta.* 413:24–32.

Lis, L. J., V. A. Parsegian, and R. P. Rand. 1981*a*. Binding of divalent

cations to dipalmitoylphosphocholine bilayers and its effect on bilayer interaction. *Biochemistry.* 20:1761–1770.

Lis, L. J., W. T. Lis, V. A. Parsegian, and R. P. Rand. 1981*b*. Adsorption of divalent cations to a variety of phosphatidylcholine bilayers. *Biochemistry.* 20:1771–1777.

Nakashima, N., S. Asakuma, J-M. Kim, and T. Kunitake. 1984. Helical superstructures are formed from the chiral ammonium bilayers. *Chem. Lett.* 1984:1709–1712.

Nakashima, N., S. Asakuma, and T. Kunitake. 1985. Optical microscopic study of helical superstructures of chiral bilayer membranes. *J. Am. Chem. Soc.* 107:509–510.

Pluta, M. 1989. Advanced Light Microscopy. Elsevier, Amsterdam.

Rhodes, D. G., S. L. Blechner, P. Yager, and P. E. Schoen. 1988. Structure of polymerizable lipid bilayers. I-1,2-bis(10,12-tricosadiynoyl)-*sn*-glycero-3-phosphocholine, a tubule-forming phosphatidylcholine. *Chem. Phys. Lipids.* 49:39–47.

Rudolph, A. S., and T. G. Burke. 1987. A Fourier-transform infrared spectroscopic study of the polymorphic phase behavior of 1,2-bis(tricosa-10,12-diynoyl)-*sn*-glycero-3-phosphocholine; a polymerizable lipid which forms novel microstructures. *Biochim. Biophys. Acta.* 902:349–359.

Servuss, R. M. 1988. Helical ribbons of lecithin. *Chem. Phys. Lipids.* 36:37–41.

Shah, D. O., and J. H. Schulman. 1965. Binding of metal ions to monolayers of lecithins, plasmalogen, cardiolipin, and dicetyl phosphate. *J. Lipid Res.* 6:341–349.

Simon, S. A., L. J. Lis, J. W. Kaufman, and R. C. MacDonald. 1975. A calorimetric and monolayer investigation of the influence of ions on the thermodynamic properties of phosphatidylcholine. *Biochim. Biophys. Acta.* 375:317–326.

Singh, A., T. G. Burke, J. M. Calvert, J. H. Georger, B. Herendeen, R. R. Price, P. E. Schoen, and P. Yager. 1988. Lateral phase separation based on chirality in a polymerizable lipid and its influence on formation of tubular microstructures. *Chem. Phys. Lipids.* 47:135–148.

Yager, P., and P. E. Schoen. 1984. Formation of tubules by a polymerizable surfactant. *Mol. Cryst. Liq. Cryst.* 106:371–381.

Yager, P., P. E. Schoen, C. Davis, R. Price, and A. Singh. 1985. Structure of lipid tubules formed from a polymerizable lecithin. *Biophys. J.* 48:899–906.

Yager, P., R. R. Price, J. M. Schnur, P. E. Schoen, A. Singh, and D. G. Rhodes. 1988. The mechanism of formation of lipid tubules from liposomes. *Chem. Phys. Lipids.* 46:171–179.

Yager, P., J. S. Chappell, and D. D. Archibald. 1991. When lipid bilayers won't form liposomes: tubules, helices, and cochleate cylinders. *In* Biomembrane Structure and Functions—The State of the Art. B. P. Gaber and K. R. K. Easwaran, editors. Adenine Press, Washington, D.C. In press.

Yamada, K., H. Ihara, T. Ide, T. Fukumoto, and C. Hirayama. 1984. Formation of helical superstructure from single-walled bilayers by amphiphiles with oligo-L-glutamate acid head group. *Chem. Lett.* 1984:1713–1716.